

Preequilibrium γ ray emission in complete and incomplete fusion reactions in the collision $^{12}\text{C}+^{64}\text{Ni}$ at 8 MeV/nucleon

F. Amorini,^{1,3} M. Cabibbo,^{1,3} G. Cardella,² A. Di Pietro,^{1,3} P. Figuera,¹ A. Musumarra,^{1,3} M. Papa,² G. Pappalardo,^{1,3} F. Rizzo,^{1,3} and S. Tudisco^{1,3}

¹*Istituto Nazionale Fisica Nucleare—Laboratorio Nazionale del Sud, Via S. Sofia 44, I-95123 Catania, Italy*

²*Istituto Nazionale Fisica Nucleare—Sezione di Catania, Corso Italia 57, I-95129 Catania, Italy*

³*Dipartimento di Fisica Universita' di Catania, Corso Italia 57, I-95129 Catania, Italy*

(Received 18 November 1997)

γ rays emitted in coincidence with charged particles have been measured in the collision $^{12}\text{C}+^{64}\text{Ni}$ at 94.7 MeV. The γ spectrum detected in coincidence with evaporation residues has been fitted using the statistical code CASCADE and does not show clear evidence for nonstatistical emission. γ spectra measured in coincidence with fast, forward emitted α particles show a contribution around 10 MeV which has been interpreted as being due to preequilibrium dipole emission in the first stages of the collision. The presence of this nonstatistical yield has been explained performing theoretical calculations based on the Boltzmann-Nordeim-Vlasov equation. [S0556-2813(98)05608-8]

PACS number(s): 24.30.Cz, 25.70.Jj

INTRODUCTION

An interesting topic in the field of heavy ion reactions is the study of γ -ray emission in the energy range $E_\gamma \approx 1-30$ MeV. Such investigations can give information on the systems produced in the collisions and on the dynamics of the reactions, e.g., Ref. [1]. In recent years, considerable efforts have been devoted to the study of the dependence of the giant dipole resonance (GDR) parameters (centroid, width, strength) on the characteristics of the emitting systems. In particular, the excitation energy and angular momentum dependence of the GDR width, e.g., Refs. [1-6] and the saturation of the GDR yield at very high excitation energies [7] have been discussed in several experimental and theoretical studies.

In addition, recent theoretical investigations [8-11] based on microscopic calculations, predict the presence, for charge asymmetric entrance channels, of a new direct mechanism of dipole emission in the energy range $E_\gamma \approx 8-15$ MeV. Such nonstatistical emission can be associated with the presence of a dipole oscillation in the first stages of the collision ($t \leq 300$ fm/c) connected to the charge equilibration dynamics. Although some experimental evidence for such preequilibrium emission exists [12-14], new experimental data are necessary for a better understanding of this effect.

In the present work we discuss some aspects of the high-energy γ -ray emission in the collision $^{12}\text{C}+^{64}\text{Ni}$ at 94.7 MeV. The chosen reaction system has a large mass asymmetry which will lead to a non-negligible component of incomplete fusion (ICF). According to the ICF systematics of the Berlin group [15] we expect to have a component of ICF $\sigma_{\text{ICF}}/(\sigma_{\text{CF}}+\sigma_{\text{ICF}}) \approx 30\%$ which also means $\sigma_{\text{ICF}}/\sigma_{\text{CF}} \approx 40\%$. Moreover due to the α structure of the ^{12}C nucleus, the ICF cross section will be dominated by the ($^{12}\text{C}, ^8\text{Be}$) and ($^{12}\text{C}, \alpha$) channels, therefore we expect to have three possible different linear momentum transfers (LMT) including complete fusion. In addition we also have a charge asymmetric entrance channel ($N/Z_{\text{targ}}-N/Z_{\text{proj}} \approx 0.29$) which should allow the presence of the above mentioned nonstatistical γ

emission, even though this effect will be weakened due to the large mass asymmetry (see, e.g., Ref. [8]). With the above points in mind, we plan to look for the presence of preequilibrium dipole emission in the studied reaction system and to investigate the possible dependence of such emission on the LMT. In the next section we will briefly discuss the experimental procedure, and in the last two sections we will present the results of the γ -residue and γ -alpha coincidences.

EXPERIMENTAL PROCEDURE

The experiment was performed at the Laboratorio Nazionale del Sud (LNS) in Catania. A self-supporting target of ^{64}Ni , 500 $\mu\text{g}/\text{cm}^2$ thick, was bombarded with a 94.7 MeV ^{12}C beam delivered by the SMP13 Tandem of the LNS. γ rays emitted in coincidence with charged particles have been detected using the TRASMA multidetector [16]. This system consists of 63 BaF_2 crystals for γ -ray detection and a ΔE - E telescope for the detection and identification of charged particles emitted at the forward angles.

The charged particle telescope, positioned 50 cm from the target, consists of an annular silicon strip (ΔE) detector (300 μm thick) divided into eight sectors followed by eight CsI crystals with photodiode readout (E). Each sector, divided into nine concentric strips, covers an angular range $\Delta\theta \approx (2^\circ-11^\circ)$ and an azimuthal angular range $\Delta\varphi \approx 45^\circ$. In the present experiment the strips of each sector have been coupled together in groups of two and the central strip has not been used. The two inner strip groups $\Delta\theta = (2^\circ-5.5^\circ)$ have been covered by a 200 μm thick Al shield which stopped the elastically scattered particles and allowed the detection of protons and α 's with thresholds of $T_p \approx 5$ MeV and $T_\alpha \approx 22$ MeV, respectively. The two outer strip groups $\Delta\theta = (6.5^\circ-10.5^\circ)$ have been used to detect light particles and heavy fragments. Protons, α 's, and evaporation residues (ER) have been identified with the time-of-flight (TOF) technique using the fast signals from the BaF_2 detectors as time references. The energy of the emitted light particles not stopped in the first stage has been obtained summing the

energies deposited in the silicon detector and in the following CsI crystals.

The BaF_2 crystals, hexagonally shaped and 6 cm large [16], were arranged into nine clusters of seven crystals each. These clusters were positioned at 45° , 90° , and 135° with respect to the beam direction at different azimuthal angles: six clusters on the horizontal plane ($\varphi=0^\circ$ and 180°) and three clusters on the vertical plane ($\varphi=90^\circ$). All the clusters were mounted 22 cm far from the target outside a small scattering chamber. Different calibration runs were performed during the experiment using standard ^{60}Co , ^{88}Y , and Am-Be sources. The use of a sum procedure among adjacent fired crystals allowed the reconstruction of the energy of the primary incident γ , improving the resolution for high-energy γ rays. Good γ - n discrimination has been obtained by combining a standard fast/slow analysis of the BaF_2 signals with the TOF measurements. The background contribution to the γ spectra in coincidence with ER and α particles has been estimated by assuming that spurious coincidences are uniformly distributed on the $E_{\text{Si-TOF}}$ identification matrix. Using this assumption, we shifted the identification gates corresponding to ER and α 's away from the correct coincidence zone and accumulated the corresponding background spectra. The background contribution obtained in this way was found to be rather small; nevertheless it was subtracted from the corresponding spectra. γ spectra measured by different clusters have been summed after Doppler shift correction. Comparisons between experimental and calculated γ spectra have been performed by folding the calculated spectra with the response functions of the BaF_2 clusters. The used response functions have been calculated, using the well known code GEANT (CERN software libraries), simulating the response of our clusters to monoenergetic γ rays isotropically emitted from the target position.

EVAPORATION RESIDUE- γ COINCIDENCES

The experimental γ spectrum in coincidence with evaporation residue is shown in Fig. 1 (open symbols). In the same figure are shown (full and dashed lines) two best fit spectra calculated using the statistical code CASCADE [17].

Before discussing the results of the statistical model fits we have to be sure that the experimental γ spectrum is only associated with complete fusion reactions. We note that ER produced in the incomplete fusion channels (^{12}C , ^8Be), and (^{12}C , α) would have energy spectra approximately centered around 2 and 7 MeV, respectively. Since the experimental energy threshold associated with the ER gate is about 7 MeV, taking into account an average energy loss in the target of about 1.5 MeV for the ER produced in the (^{12}C , α) ICF channel, we can only have a small ICF contribution in our γ spectrum. Starting from these considerations we verified, on our experimental data, that γ spectra obtained imposing larger energy thresholds on the ER are not significantly different. Therefore we concluded that the possible small contribution due to the (^{12}C , α) ICF channel has a negligible effect on the γ spectrum.

Since we are measuring γ -particle coincidence spectra, another point which has to be considered before performing a comparison with statistical model calculations, is the effect of the experimental coincidence condition on the measured γ

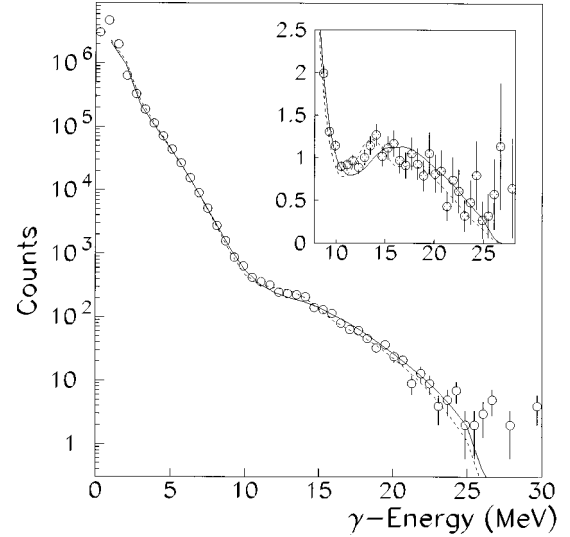


FIG. 1. γ spectrum measured in coincidence with the selected evaporation residue (open symbols). The full line is the best fit spectrum obtained with the statistical code CASCADE using a single Lorentzian for the GDR and a level density parameter $a = A/8$. The dashed line represents the best fit obtained with two Lorentzians and $a = A/8$. In the small inset the experimental data and the two fits have been divided by the same exponential factor.

spectra. As we discussed in a recent work [18], γ spectra measured in a fusion reaction in coincidence with different particles (p , α , or ER) may have a considerably different yield in the GDR region. This is due to the fact that different coincidence conditions generally select different spin distributions of the original compound nuclei (CN). We calculated the spin distribution of the original compound nuclei selected by our experimental coincidence condition using a Monte Carlo version of CASCADE [18]. This was done analyzing the event by event output file of the Monte Carlo CASCADE, and looking at the CN spin in those events leading to the emission of an ER in the angular range covered by our detector and above our experimental energy threshold. The obtained spin distribution is similar to the inclusive one. Therefore we expect that our measured GDR yield in coincidence with ER will be close to the inclusive one and a comparison with the inclusive calculation of CASCADE is justified.

The statistical model fits have been performed assuming a single and a double Lorentzian for the GDR and the results are reported in Table I. To optimize the fitting procedure, single Lorentzian fits have been performed with a fixed resonance energy (between 16.0 and 18.0 MeV) and variable values for the strength and width of the resonance. Moreover, in all the statistical model fits performed, the normalization constant between the calculated and experimental spectrum was always treated as a free parameter. Using a level density parameter $a = A/8$, we obtained the best fit at an energy $E_{\text{GDR}} = 17.0$ MeV with a width of 9.6 MeV and a strength $S = 1.4$. The errors on the extracted GDR parameters can be evaluated by looking at the fits performed with different values of the GDR centroid and are of the order of ± 0.5 MeV for the centroid, ± 1.0 MeV for the width, and ± 0.2 for the strength. The extracted value for the centroid is in good agreement with the systematics [1] which gives $E_{\text{GDR}} = 17.4$ for the mass of our compound nucleus. There

TABLE I. Results of the statistical model fits performed to reproduce the γ spectrum measured in coincidence with evaporation residue. In the two-Lorentzian fit we imposed the condition $S1 + S2 = 1$.

Kind of fit	a	$E1_{\text{GDR}}$	$E2_{\text{GDR}}$	$\Gamma1_{\text{GDR}}$	$\Gamma2_{\text{GDR}}$	$S1$	$S2$	χ^2
1 Lor.	$A/8$	17.0 ± 0.5		9.6 ± 1.0		1.4 ± 0.2		2.39
2 Lor.	$A/8$	17.8 ± 0.5	13.2 ± 0.5	7.0 ± 1.0	4.1 ± 1.0	0.6 ± 0.2	0.4 ± 0.2	1.68

are no data available in the literature for the GDR in the compound nucleus ^{76}Se at $T = 3$ MeV (i.e., our compound nucleus for complete fusion) but rather complete systematics are available for ^{63}Cu [19]. In this last reference one finds, for the collision $^{12}\text{C} + ^{51}\text{V}$, a width $\Gamma_{\text{GDR}}(^{63}\text{Cu}) \approx 10.5 \pm 0.5$ MeV at $T(^{63}\text{Cu}) \approx 2.9$ MeV which appears to be in reasonable agreement with our extracted value $\Gamma_{\text{GDR}}(^{76}\text{Se}) = 9.6 \pm 1$ MeV. The strength value extracted from the fit $S = 1.4 \pm 0.2$ is relatively large. However, taking into account the experimental error, and considering that the spin window selected by the experimental coincidence condition is not exactly equal to the inclusive one, the obtained value appears to be reasonable and in agreement with the systematics of Ref. [1]. We note that in this last reference one finds, in the vicinity of $A_{\text{CN}} = 63$, typical strength values for GDR built on excited states in the range $S = (0.8 - 1.3)$. As one can see in Fig 1 the quality of the fit (full line) is quite satisfactory. The agreement between the experimental data and the fit can be better evaluated by looking at the small insert in Fig. 1, where a linearized plot obtained by dividing the experimental data and the fits by a common exponential factor is shown.

From this linearized plot a relatively small extra yield (of the order of 10% or less) between 10 and 15 MeV seems to be present. As we will discuss in more detail later this extra yield could be a signature for the presence of nonstatistical effects, however, it can also be reproduced by using a double Lorentzian fit (dashed line in Fig. 1). In such a way the fit quality improves slightly and one finds a deformation parameter $\beta = 0.35$ and a ratio between the strengths 1.6. In our opinion, however, the large error bars on the experimental data do not allow any definite conclusion. The use of a level density parameter $a = A/9$ with a single Lorentzian does not improve the quality of the fit and gives values similar to the ones obtained with $a = A/8$.

As we discussed, the experimental spectrum can be reproduced by the statistical model calculations and there is no clear evidence for preequilibrium γ emission. Such a result can be understood by performing some theoretical calculations based on the Boltzmann-Norheim-Vlasov (BNV) equation. Details of such calculations are presented in a more general frame elsewhere [8]. Therefore in this work we will just summarize the results concerning the present colliding system. As we already discussed, we are looking for preequilibrium emission from an intermediate system which is associated with the charge equilibration process. Solving the BNV equation by means of the test particle method, it is possible to calculate the nuclear density at different times during the collision. The intermediate system can be described as divided into two subsystems and its associated total dipole can be decomposed into three terms [8]:

$$D_{\text{tot}}(t) = D_1(t) + D_2(t) + Dm(t).$$

The first two terms represent the intrinsic dipole of the two subsystems and the last term is the so-called molecular dipole whose dependence on time is associated with the charge transfer between the two subsystems during the collision. One can therefore follow the time evolution of the system and, from the Fourier analysis of the total dipole, one can obtain information on preequilibrium emission. In this way one can estimate in which energy region preequilibrium emission is expected and evaluate the associated emitted power. As an example, we show in Fig. 2 the results obtained [8] performing a BNV calculation, for the studied $^{12}\text{C} + ^{64}\text{Ni}$ collision, at an impact parameter $b = 0$. The probability of preequilibrium γ -ray emission per unit energy, shown in Fig. 2(b), is peaked around 10 MeV with a full width at half maximum (FWHM) of about 5 MeV. As one can see, we expect to have a total nonstatistical emission probability of the order of 4×10^{-5} MeV $^{-1}$ around the maximum. The statistical γ -ray emission probability per unit energy has been obtained dividing the γ spectrum calculated by CASCADE in mb (single Lorentzian fit) by the total fusion cross section. In this way we find that the nonstatistical emission probability [$Sd \approx 4 \times 10^{-5}$ MeV $^{-1}$, Fig. 2(b)] is only

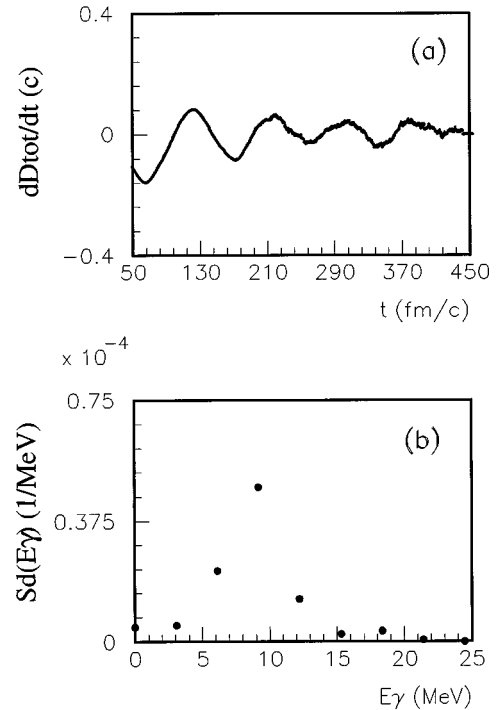


FIG. 2. (a) First time derivative of the total dipole (divided by the elementary charge e) as a function of time, obtained performing BNV calculations for the studied $^{12}\text{C} + ^{64}\text{Ni}$ collision at an impact parameter $b = 0$. (b) Corresponding probability per unit energy of preequilibrium γ -ray emission, obtained performing the Fourier analysis of the calculated total dipole.

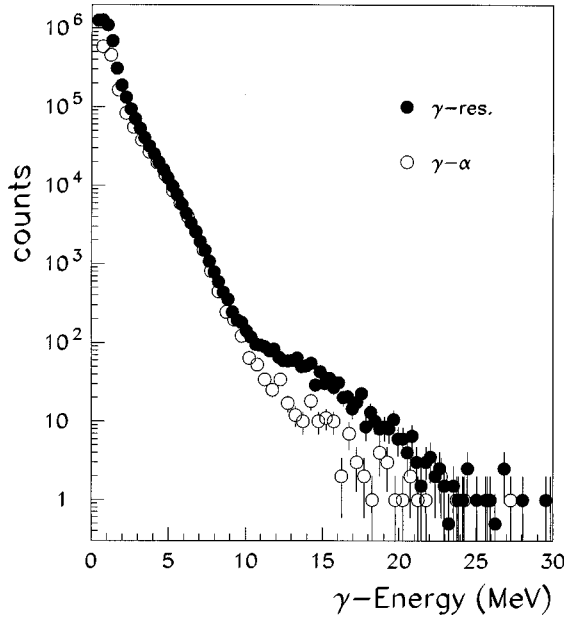


FIG. 3. Comparison between the γ spectra measured in coincidence with evaporation residues (closed symbols) and in coincidence with the α particles detected in the whole angular range covered by our telescope (open symbols). The two spectra have been normalized in the energy region $E_\gamma \approx (3-8)$ MeV.

10% or less of the probability for statistical γ -ray emission in the same energy range (e.g., $P_{\text{stat}} = 9 \times 10^{-4} \text{ MeV}^{-1}$ at $E_\gamma = 10 \text{ MeV}$, $P_{\text{stat}} = 5 \times 10^{-4} \text{ MeV}^{-1}$ at $E_\gamma = 12 \text{ MeV}$, as predicted by the CASCADE calculations). From these results we can conclude that in the studied system the preequilibrium strength cannot be clearly observed in coincidence with evaporation residues produced in complete fusion reactions because it will be easily “hidden” by the much larger statistical contribution.

α - γ COINCIDENCES

The γ spectra measured in coincidence with ER (closed symbols) and with the α particles (open symbols) detected in the whole angular range covered by our detector, are shown in Fig. 3. The two spectra have been normalized in the energy region $E_\gamma \approx (3-8)$ MeV and, as one can see from this comparison, a different relative yield in the GDR region is evident. In particular the GDR emission is suppressed as coincidences with α particles are selected. The reason for this suppression is, in principle, double. As mentioned in the previous section, in a recent work [18] we have shown how the GDR γ -ray emission can be suppressed when γ - α coincidences are selected. However, using a Monte Carlo version of CASCADE recently developed [18], we verified that in the present colliding system this effect is expected to be small. In the present case the main reason for the observed suppression in the GDR region is indeed due to the fact that most of the α particles emitted in the angular range covered by our detector are produced in incomplete fusion reactions. As we already discussed, we expect to have a ratio $\sigma_{\text{ICF}}/\sigma_{\text{CF}} \approx 40\%$. We note that both incomplete fusion channels (^{12}C , ^8Be), (^{12}C , α) produce fast forward emitted α particles, while the evaporated α 's are not very forward focused

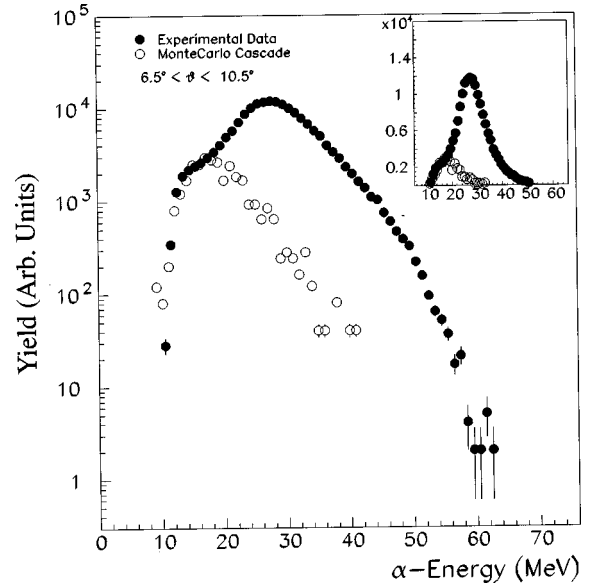


FIG. 4. Comparison between the experimental α spectrum measured in the angular range $\Delta\vartheta_{\text{lab}} = (6.5^\circ - 10.5^\circ)$ (closed symbols) and the evaporation α spectrum calculated in the same angular range (open symbols) using a Monte Carlo version of CASCADE. In the small inset the same comparison is shown on a linear scale. The two spectra have been normalized in the energy region where the calculated spectrum has its maximum.

by the kinematics due to the low c.m. velocity. The compound nuclei associated to the two ICF channels are not very different in mass from the one corresponding to CF, but they have a lower temperature thus explaining the suppression in the GDR yield. In Fig. 4 the experimental α spectrum (closed symbols) is compared with a calculation (open symbols) performed with a Monte Carlo version [18] of the evaporation code CASCADE assuming a complete fusion reaction. The experimental spectrum shows two peaks: one at $E_\alpha \approx 28 \text{ MeV}$ corresponding to α particles emitted with a velocity near to the one of the beam in incomplete fusion reactions and another peak at $E_\alpha \approx 17 \text{ MeV}$ due to fusion evaporation emission as confirmed by the comparison with the calculated spectrum. Up to now we implicitly assumed that the fast α -particle emission in the reaction channels (^{12}C , ^8Be), (^{12}C , α) is associated with an incomplete fusion mechanism, even if fast forward emitted α particles could, in principle, also be associated with a breakup mechanism not followed by incomplete fusion. In an experiment performed at the same ^{12}C incident energy on a target of similar mass (^{51}V) [20] it has been shown that the fast forward emitted α particles are associated with incomplete fusion reactions with no appreciable contribution from a breakup mechanism not followed by ICF. Therefore the assumption mentioned above can be considered correct.

From the discussion so far, we expect that a fraction of the high-energy α particles will be due to the decay of ^8Be produced in the reaction channel (^{12}C , ^8Be). The analysis of the ^8Be events has been performed by looking at the α - α coincidences between adjacent strips. In Fig. 5(a) we show the obtained $E_{\alpha 1} - E_{\alpha 2}$ spectrum where the peak corresponding to ^8Be is clearly visible. The ^8Be spectrum has been reconstructed by summing the energies of the two corresponding α particles and is shown in Fig. 5(b). As expected

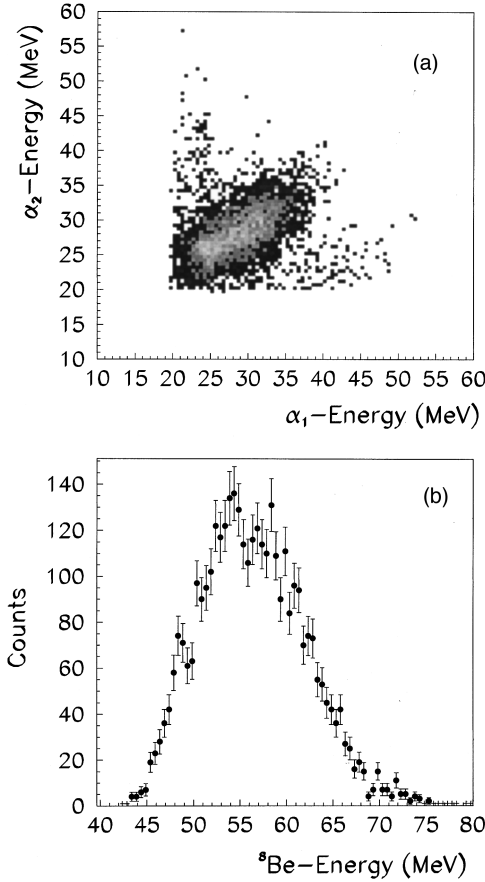


FIG. 5. (a) $E_{\alpha 1}$ - $E_{\alpha 2}$ spectrum for α particles detected in coincidence by adjacent strips. The peak at $E_{\alpha 1} \approx E_{\alpha 2}$ corresponds to the decay of a ^8Be emitted in the collision. (b) Reconstructed ^8Be spectrum obtained summing the energies of the two corresponding α particles.

the maximum yield corresponds to a ^8Be emitted with nearly beam velocity. The experimental γ spectrum measured in coincidence with ^8Be is shown in Fig. 6 (open symbols). As a comparison, in the same figure we show (full line) the result of a calculation performed with the code CASCADE in the way explained in the following. The excitation energy distribution of the ^{68}Zn reduced compound nucleus has been reconstructed starting from the ^8Be spectrum and assuming two-body kinematics obtaining $\langle E^*(^{68}\text{Zn}) \rangle \approx 35 \pm 2$ MeV. We divided the obtained distribution into different regions having an average excitation energy E_i and a corresponding number of events A_i . For each region we performed a CASCADE calculation for the ^{68}Zn reduced compound nucleus at the corresponding excitation energy E_i , and with a fixed spin J_0 independent of the excitation energy region. After that we summed the calculated γ spectra taking into account the corresponding weights $A_i/\sum A_i$. We repeated this procedure changing the spin J_0 of ^{68}Zn in order to get good agreement with the experimental data and extracted a value of the spin $J_{0(\text{exp})} \approx (12 \pm 2.0)\hbar$. These calculations have been performed using the same GDR width we extracted in the complete fusion channel and a GDR centroid given by the ground state systematics [1]. As one can see, within our statistical uncertainties the experimental spectrum appears to be well reproduced. However, we have to remark that the col-

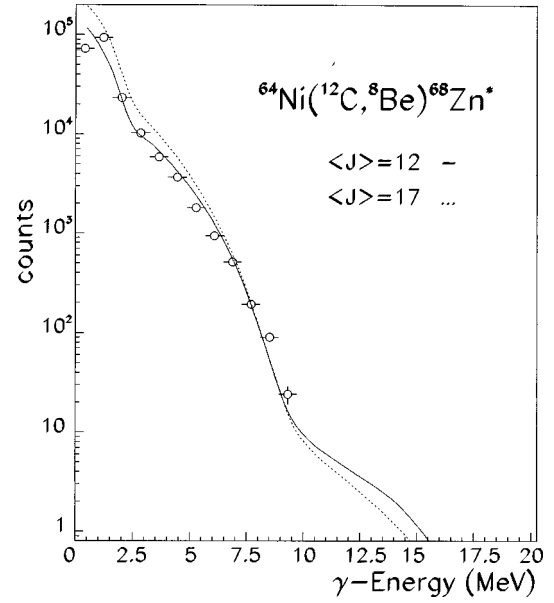


FIG. 6. γ spectrum measured in coincidence with ^8Be (open symbols). The full line is a CASCADE calculation for the ^{68}Zn reduced compound nucleus performed in the way discussed in the text with the following parameters: average spin $J_0 = 12\hbar$, $E_{\text{GDR}} = 17.8$ MeV, $\Gamma_{\text{GDR}} = 9.6$ MeV, strength = 1.2. The dashed line shows the same calculation performed with a spin $J_0 = 17\hbar$.

lected statistics is less than the one we have in the complete fusion channel (Fig. 1) and in the $(^{12}\text{C}, \alpha)$ ICF channel (Fig. 7). Therefore we cannot completely exclude the possible presence of a weak preequilibrium contribution in an energy range similar to the ones predicted for the complete fusion channel (Fig. 2) and for the $(^{12}\text{C}, \alpha)$ ICF channel (Fig. 11). In order to show the sensitivity of our CASCADE calculation to the chosen J_0 value, in Fig. 6 we also show a calculation performed with $J_0 = 17\hbar$ (dashed line). In the CASCADE calculations we just discussed, we considered a spin J_0 of the

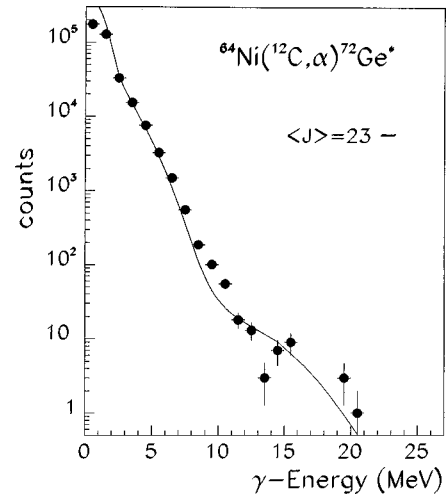


FIG. 7. γ spectrum measured in coincidence with α particles with energy $E_\alpha > 24$ MeV (closed symbols). The full line is a CASCADE calculation for the ^{72}Ge reduced compound nucleus performed in the way discussed in the text with the following parameters: average spin $J_0 = 23\hbar$, $E_{\text{GDR}} = 17.6$ MeV, $\Gamma_{\text{GDR}} = 9.6$ MeV, strength = 1.2.

^{68}Zn reduced compound nucleus independent of the excitation energy region. However, we also verified that more complex calculations taking into account the spin distribution of ^{68}Zn give as a result a mean value of the spin distribution equal to the previously found value of J_0 . The J_0 value, obtained reproducing the γ spectrum, appears to be reasonable when compared with semiclassical estimates. As a first step approximation, we used our experimental Q value ($Q_{\text{exp}} = -E^* + Q_{\text{gg}}$) in the semiclassical model for the few nucleon transfer described in Ref. [21] and based on linear and angular momenta conservation in a grazing collision. In such a way we obtain $J_0 \approx 16\hbar$ to be compared with $J_{0(\text{exp})} \approx (12 \pm 2)\hbar$. However, to be exact, one should take into account that in our case the transferred mass in a non-negligible fraction of the projectile. Using energy and angular momentum conservation and taking into account the different reduced masses in the entrance and exit channels, we were able to reproduce the transferred angular momenta only taking into account the 3α structure of the ^{12}C projectile as discussed in the Appendix. In this way we obtain a transferred angular momentum $J_0 = 13\hbar$ at an impact parameter $b \approx 5$ fm.

The experimental γ spectrum emitted in the ICF channel ($^{12}\text{C}, \alpha$) was obtained measuring γ in coincidence with α particles with $E_\alpha > 24$ MeV and is shown in Fig. 7. In this way we expect to have a negligible contribution due to complete fusion as one can see looking at the small inset in Fig. 4. To be sure, however, we verified that γ - α coincidence spectra obtained imposing larger energy thresholds on the α particles are not significantly different. Moreover we also have to estimate what fraction of the α particles measured in coincidence with the γ spectrum is due to the decay of ^8Be produced in the ($^{12}\text{C}, ^8\text{Be}$) ICF channel. In our analysis we reject all the events in which two α particles in coincidence hit the same Si strip, because the corresponding point in the $E_{\text{Si}}\text{-TOF}$ and $E_{\text{Si}}\text{-}E_{\text{CSi}}$ spectra will be outside the α identification gate. Therefore the only ^8Be contamination in our spectrum is due to α particles emitted in coincidence which do not hit the same Si strip. Starting from the coincidence events in adjacent strips, we estimated a contamination of α particles due to ^8Be decay $\alpha_{8\text{Be}}/\alpha_{\text{tot}} < 15\%$. In the analysis presented here we will always refer to the γ spectrum in coincidence with α particles of $E_\alpha > 24$ MeV, but we verified that the subtraction of a 15% ^8Be contribution does not affect our results. In Fig. 7 we also show (full line) a CASCADE calculation performed in the same way discussed for the ^8Be - γ coincidences. Once more the extracted value of the average transferred angular momentum $J_{0(\text{exp})} = (23 \pm 2.5)\hbar$ is in agreement with the two semiclassical estimations previously considered which give $J_0 = 24\hbar$ using our experimental Q value in Ref. [21] and $J_0 = 24\hbar$ at an impact parameter $b \approx 5$ fm taking into account the 3α structure of ^{12}C . Looking at Fig. 7 one can notice the presence of a contribution around $E_\gamma \approx 10$ MeV which is not reproduced by our statistical calculation. This contribution becomes evident plotting the ratio between the experimental γ spectrum and the calculated one (full line in Fig. 7) as one can see in Fig. 8. The same contribution appears when the γ spectrum in coincidence with α particles detected by the inner strips ($\Delta\vartheta = 2^\circ - 5.5^\circ$ where the preequilibrium α yield is larger) is

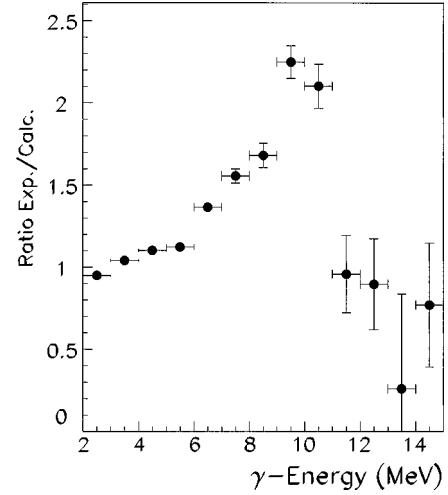


FIG. 8. Ratio between the experimental γ spectrum measured in coincidence with α particles with energy $E_\alpha > 24$ MeV and the calculated one.

compared with the γ spectrum in coincidence with α particles detected by the outer strips ($\Delta\vartheta = 6.5^\circ - 10.5^\circ$) selecting an α detection threshold of 24 MeV. Figure 9 displays the ratio between these two spectra where, once more, a peak at an energy lower than the GDR for the equilibrated system is evident. To be exact, we note that the contribution around 10 MeV can be in principle reproduced by statistical model calculations assuming a two Lorentzian splitting of the GDR. In Fig. 10 we show a comparison between the same experimental γ spectrum shown in Fig. 7 and a two Lorentzian CASCADE calculation performed in a similar way as the ones in Figs. 6 and 7. In order to reproduce the spectrum we varied the parameters $E1$, $E2$, $S1$, and $S2$ (centroids and strengths of the two components, respectively) with the constraints $S1 + S2 = 1$ and $S1 \cdot E1 + S2 \cdot E2 = \langle E \rangle$, where $\langle E \rangle = 17.6$ MeV is the GDR centroid given by the ground state systematics [1]. We used fixed values for the other parameters: spin $J_0 = 23\hbar$ (as in the calculation of Fig. 7) and

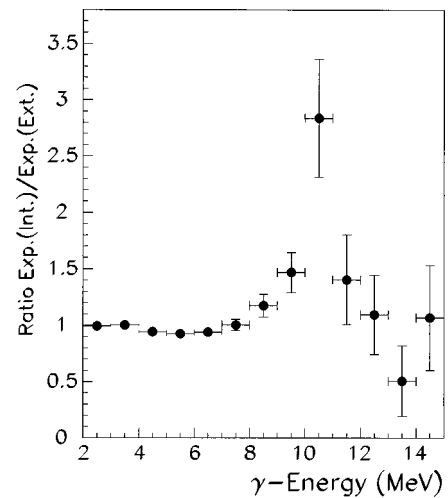


FIG. 9. Ratio between the two γ spectra measured in coincidence with α particles with energy $E_\alpha > 24$ MeV detected by the inner strips ($\Delta\vartheta_{\text{lab}} = 2^\circ - 5.5^\circ$) and in coincidence with α particles with energy $E_\alpha > 24$ MeV detected by the outer strips ($\Delta\vartheta_{\text{lab}} = 6.5^\circ - 10.5^\circ$).

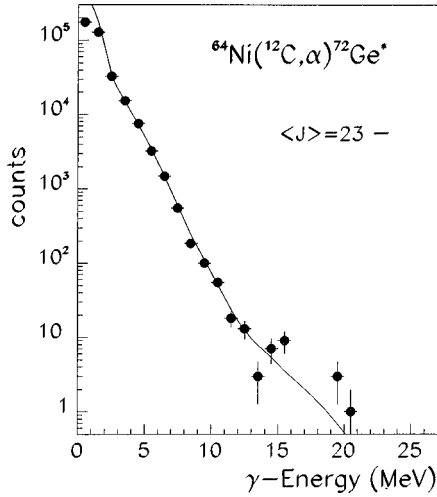


FIG. 10. Comparison between the experimental γ spectrum measured in coincidence with α particles with energy $E_\alpha > 24$ MeV (same as in Fig. 7) and a two Lorentzian CASCADE calculation performed and discussed in the text with the following parameters: $E1 = 10$ MeV, $E2 = 19.5$ MeV, $S1 = 0.2$, $S2 = 0.8$, $\Gamma1 = 3.9$ MeV, $\Gamma2 = 11.3$ MeV.

widths given by a power law on the resonance energy (e.g., Ref. [22]) $\Gamma1 = \Gamma_0(E1/\langle E \rangle)^{1.6} = 3.9$ MeV, $\Gamma2 = \Gamma_0(E2/\langle E \rangle)^{1.6} = 11.3$ MeV, where we used the width $\Gamma_0 = 9.6$ MeV extracted in the complete fusion channel. The parameters used to reproduce the spectrum (reported in the figure caption), however, would correspond to GDR emission by a prolate superdeformed nucleus with ratio between the axis $R_{\text{axis}} \approx 2$. We know that there is experimental evidence for the existence of superdeformed states in nuclei in our range of masses and spins [23] and for the emission of GDR γ rays from superdeformed nuclei [24]. However, contrary to Ref. [24] or to what is suggested in Ref. [25], our experimental coincidence condition is not very selective and GDR emission from a superdeformed nucleus does not appear to be realistic. Therefore the observed extra yield in the γ spectrum measured in coincidence with fast forward emitted α 's has been interpreted as due to the preequilibrium emission mechanism, connected with the charge equilibration process discussed in the Introduction.

Before coming to the above conclusion, we also checked the possibility of a discrete level excitation in a reaction producing fast forward emitted α particles. No reaction between ^{12}C and ^{64}Ni can reasonably give such a contribution. The only possibility could be the reaction $^{64}\text{Ni}(^{12}\text{C}, ^8\text{Be}^*)^{68}\text{Zn}^*$ but no excited state of ^8Be can decay to the ground state emitting a 10 MeV γ ray. A transition to a ^8Be excited state has also been excluded because, in this case, one would have a larger relative angle between the two α particles coming from the ^8Be decay. In such a case the observed extra yield should be present, in the same way, in coincidence with α 's detected by the inner and also by the outer strips, while we observe a larger yield for the inner strips. From the analysis of the elastic scattering spectra (measured without γ coincidence condition in the acquisition trigger) we know that a small contamination of ^{12}C is present in the target. Therefore, in order to be sure, we also have to exclude possible $^{12}\text{C} + ^{12}\text{C}$ reactions. The possibility to populate discrete levels of ^{16}O and ^{20}Ne by means of the reactions

$^{12}\text{C}(^{12}\text{C}, ^8\text{Be})^{16}\text{O}$ and $^{12}\text{C}(^{12}\text{C}, \alpha)^{20}\text{Ne}$ has been investigated. For the isospin conservation rule only levels with $T=0$ have been taken into account. Moreover since the γ peak is observed in coincidence with forward emitted α particles, for parity and angular momentum conservation we have to look for states with natural parity [26]. The number of levels satisfying the above mentioned conditions is small (e.g., Refs. [27–29]) and, in addition, the spin and parity of these levels do not allow a transition with $E_\gamma \approx 10$ MeV. From the above considerations, the possibility of a discrete level excitation in reactions producing fast forward emitted α particles can be reasonably excluded.

In a similar way to that discussed for the γ -residue coincidences, we tried to understand our experimental results performing BNV calculations. Normally such calculations are not able to reproduce fast forward emitted α particles for the collision studied here. Increasing the impact parameter value one finds fusion up to $b \approx 7$ fm and at larger b values a quasiprojectile is produced. In order to reproduce our data, as discussed in detail in Ref. [8], we have tried to simulate in the semiclassical calculations a 3α clustered ^{12}C projectile. We know from spectroscopy studies that excited states of ^{12}C around 10 MeV have been described by a prominent 3α structure having an equilateral triangular shape (e.g., Refs. [30–32]). Starting from this consideration we prepared the initial state of the ^{12}C for the BNV calculation distributing test particles around the vertex of an equilateral triangle in order to simulate a clustered ^{12}C projectile. The orientation of the 3α triangle has been chosen to minimize the Coulomb interaction with the target. As an example, starting from this configuration at an impact parameter $b = 4.7$ fm we find that a transfer of two α particles takes place in about 250 fm/c, and we observe an α particle having an energy of about 6.5 MeV/nucleon in the outgoing channel. In Fig. 11 the first time derivative (divided by the elementary charge e) of total (a) and molecular (b) dipoles, defined in the previous sections, are reported versus time. One can see that the molecular dipole is a large fraction of the total dipole. This confirms the connection between the preequilibrium dipole emission and the transfer of charge between the partners of the collision. As shown in Fig. 11(c), the Fourier analysis of the total dipole gives a strength centered at about 13 MeV with a width of about 3 MeV in qualitative agreement with the experimental findings. The calculated probability for preequilibrium γ emission around the maximum is twice the probability for the complete fusion case. At the same time, in the energy region where the experimental preequilibrium γ yield is present, the probability for statistical γ -ray emission (calculated with CASCADE in the same way explained in the previous section) is half the probability of the complete fusion case. Therefore, according to these theoretical estimates, it should be easier to experimentally observe the preequilibrium yield in the selected ICF channel. We experimentally find that the preequilibrium γ -emission probability is of the same order of the statistical one around $E_\gamma = 10$ MeV (see Fig. 8). At this energy, the ratio between the number of counts in the extra yield and the number of events which triggered the γ spectrum is $P_{\text{exp}} \approx 2 \times 10^{-4}$. This approximate experimental estimation of the preequilibrium emission probability is of the same order of the calculated preequilibrium emission probability at the maximum as one can see in

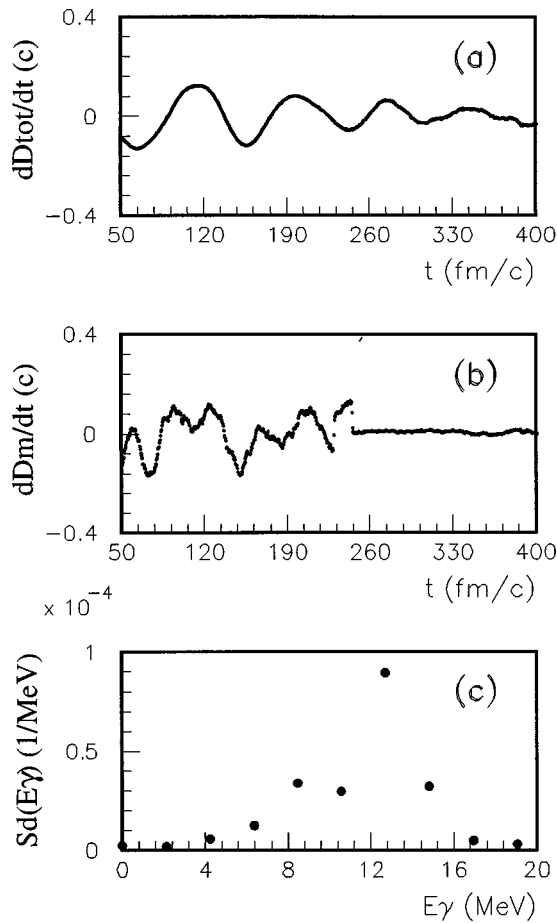


FIG. 11. First time derivative (divided by the elementary charge e) of the total dipole (a) and of the molecular dipole (b) as function of the time obtained simulating a 3α clustered ^{12}C projectile in a BNV calculation. (c) Corresponding probability per unit energy of preequilibrium γ -ray emission obtained performing the Fourier analysis of the calculated total dipole.

Fig. 10. From these results one could conclude that in the particular reaction channel considered there is a short time interval where the preequilibrium effects are the prominent ones, and the reaction channel selection performed appears to be well suited to the experimental observation of such preequilibrium effects.

SUMMARY AND CONCLUSIONS

In this work we discussed some aspects of the γ -ray emission in the collision $^{12}\text{C} + ^{64}\text{Ni}$ at 94.7 MeV.

The γ spectrum detected in coincidence with evaporation residues produced in complete fusion reactions is well reproduced by statistical model calculations and shows no clear evidence for preequilibrium dipole emission. The GDR parameters extracted by the statistical model fit are in agreement with the available data for emitting systems of similar masses and temperatures. BNV calculations predict a probability per unit energy of preequilibrium dipole emission which is only 10% or less of the probability for statistical emission in complete fusion. Therefore, in this range of excitation energies and masses, the detection of γ rays in coincidence with evaporation residues produced in complete fu-

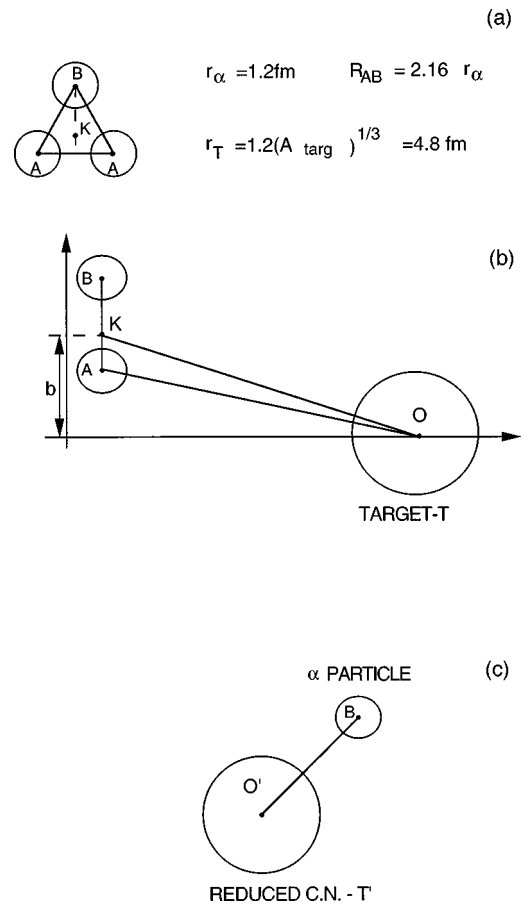


FIG. 12. (a) The 3α structure of ^{12}C considered in our semiclassical calculations: 3α particles are at the vertex (A,A,B) of an equilateral triangle, K is the center of mass of the ^{12}C projectile, r_α is the α particle radius (half density radius), r_T is the target radius, and R_{AB} is the distance between two vertexes. (b) Entrance channel configuration: the 3α plane is normal to the beam direction (horizontal) and one of the vertex is in the direction of the impact parameter b . (c) Exit channel configuration after a ^8Be transfer: T' is the reduced compound nucleus.

sion reactions is not well suited to the observation of preequilibrium effects.

Contrary to the complete fusion case, a nonstatistical contribution has been found in the γ spectra measured in coincidence with fast forward emitted α particles produced in incomplete fusion reactions. This behavior can be explained by BNV calculations which simulate a 3α clustered ^{12}C projectile. We found that in the particular outgoing channel considered there is a short time interval where the preequilibrium effects are the prominent ones. Therefore, according to the obtained results, the experimental observation of preequilibrium effects appears to be strongly connected to the selected reaction mechanism.

ACKNOWLEDGMENTS

The authors wish to thank Dr. T. Davinson for useful suggestions and V. Campagna and S. Salomone for technical help during the experiment.

APPENDIX

As we already discussed, it has been shown by spectroscopic studies that the first excited states of ^{12}C can be de-

scribed by a prominent 3α structure having an equilateral triangular shape. We discussed how we included this 3α structure in our BNV calculations. Moreover, with classical considerations, we also estimated the transferred angular momentum in the (^{12}C , ^8Be) and (^{12}C , α) channels taking into account the 3α structure of the ^{12}C projectile. In the following, as an example, we will discuss the case of the (^{12}C , α) channel with the help of Fig. 12. Given two generic points X, Y , we will indicate R_{XY} the distance between these points: V_{XY}^{\parallel} , the component of the velocity along the direction XY and V_{XY}^{\perp} , the component of the velocity normal to the direction XY .

As shown in Fig. 12(b), in the entrance channel we assume the 3α plane normal to the beam direction and with one of the vertex (B in the figure) along the direction of the impact parameter b . This configuration minimizes the Coulomb repulsion between projectile and target. In the final channel [Fig. 12(c)] we will have a reduced compound nucleus T' and an emitted α particle. We assume that the transfer takes place when $R_{AO} = r_{\alpha} + r_T$ with a relative velocity $V_{OA}^{\parallel} = 0$. For the conservation of angular momentum we can write

$$\mu_i * V_{OK}^{\perp} * R_{OK} = J_0 + \mu_f * V_{O'B}^{\perp} * R_{O'B}.$$

Here μ_i and μ_f are the initial and final reduced masses and J_0 is the transferred angular momentum. The energy conservation can be expressed as

$$\begin{aligned} 1/2 \mu_i [(V_{OK}^{\parallel})^2 + (V_{OK}^{\perp})^2] + V_i \\ = 1/2 \mu_i [(V_{O'B}^{\parallel})^2 + (V_{O'B}^{\perp})^2] + V_f + E^* + Q_{gg}. \end{aligned}$$

Here $V_i = 2 * (Z_{\alpha} Z_T) / (r_{\alpha} + r_T) + (Z_{\alpha} Z_T) / (R_{OB})$ is the Coulomb barrier in the initial configuration, $V_f = (Z_{\alpha} Z_{T'}) / (r_{\alpha} + r_{T'})$ is the Coulomb barrier in the final configuration, E^* is the excitation energy, and Q_{gg} is the ground state Q value. In addition we verified that from the assumption that the transfer takes place with a relative velocity $V_{OA}^{\parallel} = 0$, it follows that the term $\frac{1}{2} \mu_f (V_{O'B}^{\parallel})^2$ in the final channel energy can be neglected within a few percent. Combining the two obtained equations, we obtained the calculated value of J_0 which has been previously reported together with the corresponding value of the impact parameter b . Following an analogous procedure we also calculated the transferred angular momentum in the (^{12}C , α) ICF channel.

-
- [1] J. J. Gaardhoje, *Annu. Rev. Nucl. Part. Sci.* **42**, 483 (1992), and references therein.
 - [2] M. Mattiuzzi, A. Bracco, F. Camera, W. E. Ormand, J. J. Gaardhoje, A. Maj, B. Million, M. Pignatelli, and T. Tveter, *Nucl. Phys.* **A612**, 262 (1997).
 - [3] E. Ramakrishnan *et al.*, *Phys. Rev. Lett.* **76**, 2025 (1996).
 - [4] M. Mattiuzzi, A. Bracco, F. Camera, B. Million, M. Pignatelli, J. J. Gaardhoje, A. Maj, T. Ramsøy, T. Tveter, and Z. Zelazny, *Phys. Lett. B* **364**, 13 (1995).
 - [5] H. J. Hofmann, J. C. Bacelar, M. N. Harakeh, T. D. Poelheken, and A. van der Woude, *Nucl. Phys.* **A571**, 301 (1994).
 - [6] G. Enders *et al.*, *Phys. Rev. Lett.* **69**, 249 (1992).
 - [7] P. Piattelli *et al.*, *Nucl. Phys.* **A599**, 63c (1996), and references therein.
 - [8] M. Papa, F. Amorini, M. Cabibbo, G. Cardella, A. Di Pietro, P. Figuera, A. Musumarra, G. Pappalardo, F. Rizzo, and S. Tuddisco, in *Proceedings of the International Conference on Nuclear Reaction Mechanisms*, Varenna, 1997 (unpublished); *Eur. Phys. J.* (to be published).
 - [9] V. Baran, M. Colonna, M. Di Toro, A. Guarnera, and A. Smerzi, *Nucl. Phys.* **A600**, 111 (1996).
 - [10] Ph. Chomaz, M. Di Toro, and A. Smerzi, *Nucl. Phys.* **A563**, 509 (1993).
 - [11] C. Yanhuang, M. DiToro, M. Papa, A. Smerzi, and Z. Jiquan, in *Proceedings of the International Conference on Dynamical Features of Nuclei and Finite Systems*, Barcelona, 1993, edited by X. Vinas (unpublished).
 - [12] V. V. Kamanin, A. Kugler, Yu. G. Sobolev, and A. S. Fomichev, *Z. Phys. A* **337**, 111 (1990).
 - [13] L. Campajola *et al.*, *Z. Phys. A* **352**, 421 (1995).
 - [14] S. Flibotte *et al.*, *Phys. Rev. Lett.* **77**, 1448 (1996).
 - [15] H. Morgenstern, W. Bohne, W. Galster, K. Grabisch, and A. Kyanowski, *Phys. Rev. Lett.* **52**, 1104 (1984).
 - [16] A. Musumarra *et al.*, *Nucl. Instrum. Methods Phys. Res. A* **370**, 558 (1996).
 - [17] F. Puhlhofer, *Nucl. Phys.* **A280**, 267 (1977).
 - [18] M. Cabibbo, Ph.D. thesis, University of Catania, 1997; F. Rizzo *et al.*, in *Proceedings of the International Conference on Nuclear Reaction Mechanisms* [8].
 - [19] M. Kicinska-Habior, K. A. Snover, C. A. Gosset, J. A. Behr, G. Feldmann, H. K. Glatzel, J. H. Gundlach, and E. F. Garman, *Phys. Rev. C* **36**, 612 (1987).
 - [20] D. J. Parker, J. Asher, T. W. Conlon, and I. Naqib, *Phys. Rev. C* **30**, 143 (1984).
 - [21] R. G. Satchler, *Direct Nuclear Reactions* Vol. 68 of *International Series of Monographs on Physics* (Oxford University Press, Oxford, 1983), p. 702.
 - [22] Y. Alhassid and B. Bush, *Nucl. Phys.* **A509**, 461 (1990).
 - [23] A. Macchiavelli, in *Proceedings of the International Symposium on Exotic Nuclear Shapes*, Debrecen, Hungary, 1997 [*Acta Phys. Acad. Sci. Hung.* **6**, 219 (1997)].
 - [24] A. Bracco *et al.*, in *Proceedings of the International Symposium on Exotic Nuclear Shapes* [23], p. 83.
 - [25] F. Bourguin *et al.*, *Phys. Rev. C* **56**, 3180 (1997).
 - [26] O. Hausser, T. K. Alexander, A. B. McDonald, G. T. Ewan, and A. E. Litherland, *Nucl. Phys.* **A168**, 17 (1971).
 - [27] L. R. Greenwood, R. E. Segel, K. Raghunathan, M. A. Lee, H. T. Fortune, and J. R. Erskine, *Phys. Rev. C* **12**, 156 (1975).
 - [28] E. Mathiak, K. A. Eberhard, J. G. Cramer, H. H. Rossner, J. Stettmeier, and A. Weidinger, *Nucl. Phys.* **A259**, 129 (1976).
 - [29] E. T. Mirgule, S. Kumar, M. A. Eswaran, D. R. Chakrabarty, V. M. Datar, N. L. Ragoowansi, H. H. Oza, and W. K. Pal, *Nucl. Phys.* **A583**, 287 (1995).
 - [30] Hisashy Horiuky *et al.*, *Prog. Theor. Phys. Suppl.* **52**, 89 (1972).
 - [31] Y. Abe, J. Hiura, and H. Tanaka, *Prog. Theor. Phys.* **49**, 800 (1973); *Prog. Theor. Phys. Suppl.* **52**, 228 (1972).
 - [32] D. M. Brink, *Proceedings of the International School of Physics "Enrico Fermi," Course XXXVI* (1966), p. 247.